NMR study of structure and electron transfer mechanism of Pseudomonas aeruginosa azurin

Groeneveld, C.M; Canters, G.W.

THE JOURNAL OF BIOLOGICAL CHEMISTRY
Vol. 263, No. 1, Issue of January 5, pp. 167-173, 1988
Printed in U.S.A.

NMR Study of Structure and Electron Transfer Mechanism of *Pseudomonas aeruginosa* Azurin*

(Received for publication, June 30, 1987)

Cornelis M. Groeneveld and Gerard W. Canters‡

From the Gorlaeus Laboratories, Leiden University, P. O. Box 9502, 2300 RA Leiden, The Netherlands

The nuclear spin-spin and spin-lattice relaxation times of the $C_{\epsilon 1}$-proton of His-35 and the $C_{\delta 2}$-proton of His-46 of reduced *Pseudomonas aeruginosa* azurin have been determined at 298 and 320 K and at pH 4.5 and 9.0 at various concentrations of total azurin and in the presence of varying amounts of oxidized azurin. The relaxation times appear strongly influenced by the electron self-exchange reaction between oxidized and reduced protein. The T_1 data of the His-35 proton have been analyzed according to the "fast-exchange limit," while the "slow-exchange limit" appears to obtain for the T_2 data of the His-46 proton. Analysis of the proton relaxation data yields values of the electron self-exchange rate constants of $(9.6 \pm 0.7) \times 10^5$ M^{-1} s^{-1} (pH 4.5) and $(7.0 \pm 1.3) \times 10^5$ M^{-1} s^{-1} (pH 9.0) at 298 K. The dipolar correlation time amounts to 1–2.5 ns in the temperature range of 298–320 K. A Fermi-contact interaction of about 100 mG for the $C_{\delta 2}$-proton of His-46 is compatible with the experimental observations. The pH-induced conformational changes lead to variations on the order of about 1 Å in the distance from the copper to the His-35 protons. The data implicate the "hydrophobic patch" around His-117 as the site of electron transfer in the self-exchange reaction of the azurin.

Electron self-exchange reactions of redox proteins receive considerable attention at the moment. Not only do electron self-exchange rates figure prominently in the Marcus theory of electron transfer (Marcus, 1963), but the study of this type of reaction may also give new insight into the electron transfer mechanism of redox proteins (Cho *et al.*, 1984; Groeneveld and Canters, 1985a). In addition, there is a number of practical advantages in studying self-exchange reactions. For instance, the absence of a driving force facilitates the theoretical analysis of experimental data. Also, for the interpretation of kinetic data the structural details of only one protein are needed.

Despite their theoretical and practical importance, electron self-exchange rates have been determined directly for only a few redox proteins. Apart from a few cytochromes (Gupta *et al.*, 1972; Keller and Wüthrich, 1976; Concar *et al.*, 1986), the self-exchange rates of a limited number of blue-copper proteins have been reported (Beattie *et al.*, 1975; Dahlin *et al.*, 1984). In the case of azurin, the blue-copper protein of *Pseudomonas aeruginosa* on which the present study focuses, there is the added and interesting complication of the purported pH dependence of the redox activity as observed in reactions with partners like cytochrome c_{551} (Silvestrini *et al.*, 1981) and derivatives of flavocytochrome b_2 (Silvestrini *et al.*, 1986). Regarding this pH dependence, it has become clear that a change in pH effects a change in the conformation of the *P. aeruginosa* azurin (Adman *et al.*, 1982, 1983), but it has proven difficult, until now, to quantify the extent of this change. Moreover, it is not clear at all whether this conformational change is related to the variation in redox activity of the protein and, if so, in what manner (Corin *et al.*, 1983).

A related question concerns the actual mechanism of electron transfer. The redox active copper center is located some distance from the protein's surface (>7 Å) (Adman *et al.*, 1978; Adman and Jensen, 1981), and it is an intriguing question how electrons travel from the outside of the protein to the metal and vice versa.

A study of the electron self-exchange reaction may provide important clues to these questions. Self-exchange rates extracted from a Marcus analysis of the electron transfer reactions of azurin with various transition metal complexes yielded values varying from 2.6×10^{-3} M^{-1} s^{-1} to 6.3×10^5 M^{-1} s^{-1} (Canters and Groeneveld, 1986; Farver and Pecht, 1981c). On the other hand, preliminary values of the *directly* determined self-exchange rate vary from 10^4 to 10^6 M^{-1} s^{-1} (Ugurbil and Mitra, 1985; Groeneveld and Canters, 1985a, 1985b). The latter value seems exorbitantly high at first sight, in view of the electron travel distance of at least 14 Å. An unambiguous, reliable determination of the electron self-exchange rate of azurin seems, therefore, to be in order. Also, the pH dependence of the self-exchange rate may shed light on the mechanism governing the pH dependence of the protein's redox activity.

In this paper, an accurate determination of the electron self-exchange rate of *P. aeruginosa* azurin at different pH values is reported. The determination is based on a study of the paramagnetic relaxation effects that can be observed in the ^1H NMR spectrum of a slightly oxidized solution of the reduced protein. The effects have been studied in detail for the T_1 and T_2 relaxation times of protons of two histidines, which are closely connected with the pH dependence of the azurin conformation and the coordination of the metal, *viz.* His-35 and His-46.

It will be shown how a consistent analysis of all relaxation data can be performed and how the analysis provides for a self-exchange rate constant on the order of 10^6 M^{-1} s^{-1} at room temperature. The analysis of the relaxation data also provides for a quantification of the structural effects on His-35 induced by a change of pH. A remarkable observation is that the structural effects of a pH change are considerable, while the effect of pH on the self-exchange rate is negligible. Combination of all of the experimental data, however, provides for a plausible model for the electron self-exchange mechanism, as discussed at the end of the paper.

* The costs of publication of this article were defrayed in part by the payment of page charges. This article must therefore be hereby marked "*advertisement*" in accordance with 18 U.S.C. Section 1734 solely to indicate this fact.

‡ To whom correspondence should be addressed.

MATERIALS AND METHODS

Protein Preparation and Handling—Azurin was isolated from *P. aeruginosa* bacterial paste and purified as described earlier (Ambler, 1963; Parr *et al.*, 1976). The ratio of the absorbances at 625 and 280 nm was used as a measure of the purity of the azurin (Ambler, 1963; Parr *et al.*, 1976) and usually amounted to 0.56. NMR sample preparation and sample handling were performed as described earlier (Groeneveld and Canters, 1985a, 1985b).

Total azurin concentrations were measured spectrophotometrically by determining the absorbance of the oxidized protein in solution at 625 nm (ϵ_{625} = 5700 M^{-1} s^{-1} (Goldberg and Pecht, 1976)). The total azurin concentrations of the NMR samples were between 1 and 4.5 mM.

The concentration of the paramagnetic species in the partly oxidized samples was measured with a special sample holder that allows the absorbance of the solution in the NMR tube to be measured at 625 nm on a Cary-219 UV/VIS spectrometer. The concentration was measured before and after each NMR experiment, and the average of the two values was used in the calculations.

NMR Measurements—NMR spectra were measured on a Bruker WM-300 spectrometer at 298 and 320 K. Free induction decays were accumulated in 8K memory and Fourier-transformed in 16K memory after zero filling.

T_1 measurements were performed by the inversion recovery procedure. The peak heights obtained from the spectra were used for a two-parameter nonlinear least squares fit to a single exponential to obtain the T_1 value. T_2 values were obtained by multiplying line widths at half-height by π.

Quoted chemical shifts are in parts per million downfield from sodium 2,2-dimethyl-2-silapentane 5-sulfonate.

RESULTS

Relaxation Data—The spin-lattice and spin-spin relaxation times (T_1, T_2) of the $C_{\epsilon 1}$-proton of His-35 at δ = 9.43 ppm (pH 4.5) or δ = 8.06 ppm (pH 9.0) and the $C_{\delta 2}$-proton of His-46 at δ = 5.55 ppm (pH 4.5) or δ = 5.88 ppm (pH 9.0) were measured as a function of the concentration of (paramagnetic) oxidized azurin at different temperatures (298 and 320 K), different total azurin concentrations (1 and 4.5 mM), and different pH values (4.5 and 9.0). The pH dependence of the imidazole resonance positions is connected to conformational changes of the protein (Adman *et al.*, 1982, 1983; see below) and does not influence the relaxation measurements. An example of a measurement is shown in Figs. 1 and 2.

Fig. 1 shows the results of two T_1 experiments, one performed on a fully reduced azurin solution (*left*, Fig. 1) and one on a partly oxidized azurin solution (*right*, Fig. 1), both at pH 9.0, 298 K, and at a total azurin concentration, [Az_t], of 1 mM. The effect of the introduction of the paramagnetic particles is clearly observable as a drastic shortening of the spin-lattice relaxation time of the His-46 proton, an effect that is much less pronounced for the His-35 proton and almost absent for the His-83 proton.

Fig. 2 shows the effects of an increase of the amount of oxidized azurin on the spin-spin relaxation time of the imidazole protons of the different histidine residues as a pronounced line broadening, which again appears to be different for the different protons.

The paramagnetic effects on the spin-spin and spin-lattice relaxation times were analyzed by plotting T_i^{-1} (i = 1, 2) *versus* [Az_{ox}], the oxidized azurin concentration. An example is shown in Fig. 3 for the measurements at pH 9.0, 298 K, and [Az_t] = 4.5 mM. As will be discussed in the next section, the important parameter is the slope of this plot, s_i, (i = 1, 2). Values of s_i are presented in Table I for the His-35 and His-46 protons. The last two columns of Table I, to be discussed in the next section, denote the relaxation regimes of the T_1 and T_2 data.

Data Handling—The present study deals with the effects of small amounts of (paramagnetic) oxidized protein on the

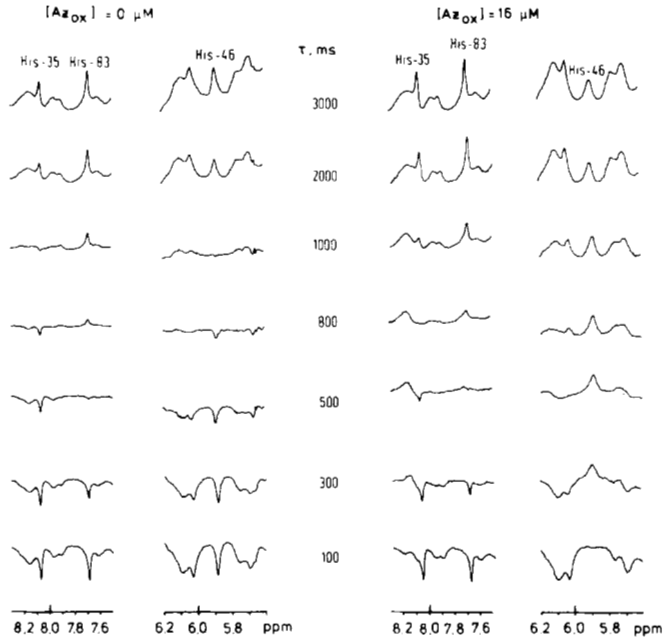

FIG. 1. **Regions of the 300-MHz NMR spectrum of a fully reduced (*left*) and a partly oxidized protein solution (*right*; [Az_{ox}] = 16 μM) as employed for the T_1 measurements at pH = 9.0 and T = 298 K.** Total azurin concentration amounts to 1 mM. Spectra were obtained with a 180 °-τ_D-90 ° pulse sequence. From *top* to *bottom*, the delay time τ_D decreases from 3000 to 100 ms.

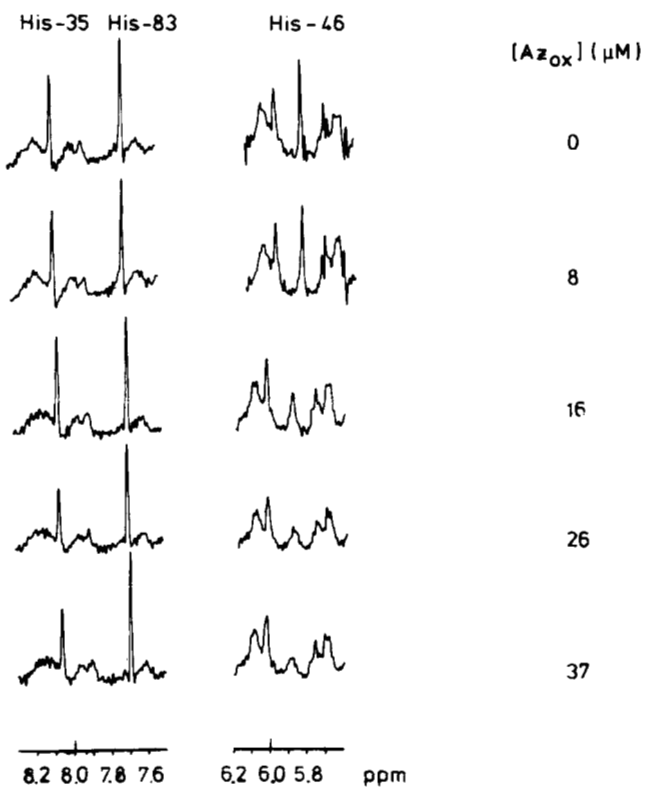

FIG. 2. **NMR spectra showing the different histidine resonances that were used for the T_2 experiments.** Conditions: 20 mM borate buffer, pH = 9.0, T = 298 K, and [Az_t] = 1 mM. From *top* to *bottom*, the oxidized azurin concentration increases from 0 to 37 μM.

NMR spectrum of the reduced species. That these effects can been seen at all is a direct consequence of the electron exchange reaction between the reduced and oxidized species. Due to this exchange, the nuclei in the reduced protein experience a magnetic perturbation each time the protein becomes oxidized. This perturbs the motion of the nuclear spins. In practice, two limiting situations are of importance. In the fast-exchange limit, the electron exchange is so fast that, experimentally, an average is observed of the spectra of the diamagnetic and the paramagnetic species. In the slow-exchange limit, the magnetic perturbations are so large that the phase coherence of the nuclear spins is destroyed, and the spin relaxation is effectively governed by the average lifetime of the molecule in the diamagnetic state. Because the application of the proper limit is crucial for the outcome of the analysis, the phenomenological characteristics of the slow- and fast-exchange limit are derived first. Subsequently, under "Discussion," the relaxation regimes (fast and slow exchange) will be investigated for the His-35 and His-46 proton spins, and on the basis of this a numerical analysis will be presented.

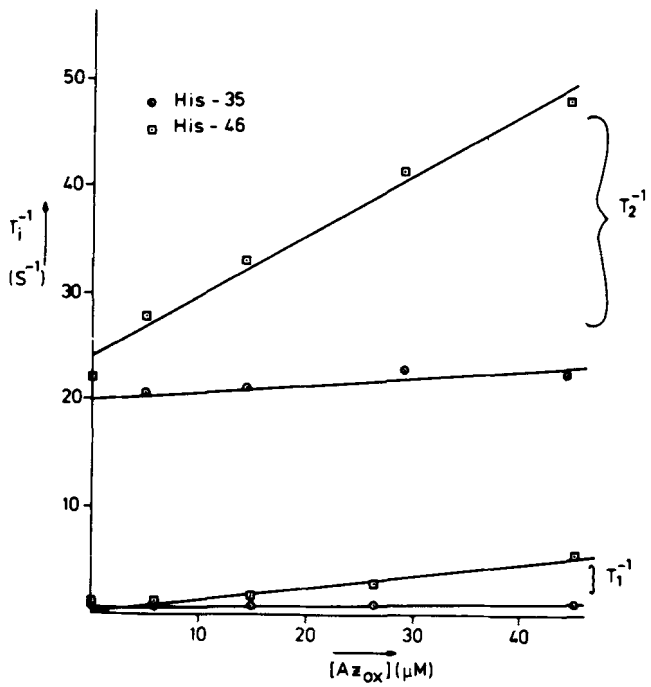

FIG. 3. **Plot of T_i^{-1} (i = 1,2) (s^{-1}) *versus* [Az_{ox}] (μM) for the His-35 and His-46 proton.** Measurements were performed at pH 9.0, T = 298 K and [Az_t] = 4.5 mM.

The present treatment is based on the work of McLaughlin and Leigh, 1973. The two cases that are relevant here are those of the "slow exchange" and the "fast exchange with exchange narrowing," the latter one being denoted by "fast exchange" in this paper. The conditions for which these limiting cases obtain are

$$k[Az_t] \ll T_{i,p}^{-1} \text{ (slow-exchange limit)} \quad (1a)$$

$$k[Az_t] \gg T_{i,p}^{-1} \text{ (fast-exchange limit)} \quad (1b)$$

[Az_t] representing the total azurin concentration, k the second order electron self-exchange rate constant, while $T_{i,p}^{-1}$ (i = 1, 2) is given by $T_{i,p}^{-1} = T_{i,ox}^{-1} - T_{i,r}^{-1}$. The subscripts ox and r denote the oxidized and reduced species, respectively. Thus, $T_{i,p}^{-1}$ represents the contribution to the proton relaxation time in the oxidized species, which is due to the paramagnetism of the unpaired electron. (Notice that when the slow-exchange limit condition applies for the T_1 data, it must also hold for the T_2 data. On the other hand, when the fast-exchange limit obtains for the T_2 data, it also holds for the T_1 data. This follows from Equation 1 and the generally valid inequality $T_2^{-1} \geqq T_1^{-1}$).

The expressions for the proton spin relaxation times corresponding with the conditions of Equation 1, a and b, are

$$T_i^{-1} = T_{i,r}^{-1} + k[Az_{ox}] \text{ (slow-exchange limit)} \quad (2a)$$

$$T_i^{-1} = T_{i,r}^{-1} + \frac{T_{i,p}^{-1}}{[Az_t]}[Az_{ox}] \text{ (fast-exchange limit)} \quad (2b)$$

in which [Az_{ox}] denotes the concentration of the oxidized azurin. When plotting T_i^{-1} as a function of [Az_{ox}], the slope of the regression line, s_i, directly provides an estimate of k (slow-exchange limit) or an estimate of $T_{i,p}^{-1}/[Az_t]$ (fast-exchange limit).

$$s_i = k \text{ (slow-exchange limit)} \quad (3a)$$

$$s_i = T_{i,p}^{-1}/[Az_t] \text{ (fast-exchange limit)} \quad (3b)$$

Examples of such plots have been presented in Fig. 3. Values of s_i obtained for a variety of experimental conditions have been collected in Table I.

From Equation 2, a number of characteristics of the slow- and fast-exchange limit can be derived to establish which limit applies in a particular case. These are discussed below in terms of the effects of various parameters on the slopes s_i.

Effect of Temperature—The electron self-exchange of blue-

TABLE I

Relaxation data for the protons of His-35 and His-46

	T	pH	[Az_t]	s_1	s_2	s_2/s_1	Relaxation regime[a]	
							T_1	T_2
	K		mM	$\mu M^{-1} s^{-1}$				
His-35	298	4.5	1	0.062 (0.006)	0.23 (0.02)	3.7 (0.5)	f	i
		9.0	1	0.027 (0.003)	0.12 (0.04)	4.4 (1.6)	f	f
			4.5	0.0055 (0.0013)	0.061 (0.019)	11.1 (4.3)	f	f
	320	4.5	1	0.060 (0.003)	0.48 (0.07)	8.1 (1.2)	f	f
		9.0	4.5	0.0056 (0.0009)	0.08 (0.05)	14.6 (9.6)	f	f
His-46	298	4.5	1	0.70 (0.21)	0.96 (0.07)	1.4 (0.4)	s	s
		9.0	1	0.48 (0.06)	0.70 (0.13)	1.5 (0.3)	s/i	s
			4.5	0.11 (0.01)	0.57 (0.04)	5.3 (0.8)	f	s
	320	4.5	1	0.60 (0.25)	3 (1)[b]	5.0 (2.7)	f	s
		9.0	4.5	0.11 (0.01)	1.0 (0.1)	9.1 (1.2)	f	i

[a] f, fast; i, intermediate; s, slow.
[b] Estimated error.

copper proteins is often characterized by a sizable activation energy. Consequently, a rise in temperature is usually accompanied by a substantial increase of the rate constant. On the other hand, the temperature dependence of $T_{i,p}^{-1}$ is governed by the much smaller activation energies of the electron spin and rotational correlation times. A rise in temperature of 10 or 20 °C, in this case, will result in a slight or negligible decrease of $T_{i,p}^{-1}$. The slow- and fast-exchange limits, therefore, exhibit different temperature characteristics, *i.e.* in the slow-exchange limit, s_i will increase markedly with temperature, while in the fast-exchange limit, s_i will show a slight decrease or will hardly be affected at all.

Effect of [Az$_t$]—As Equation 3 shows, the absence of an effect of the total azurin concentration [Az$_t$] on the slope s_i is compatible with the slow-exchange limit, while in the fast-exchange case the slope is proportional to $[Az_t]^{-1}$.

Ratio s_2/s_1—The ratio of s_2 and s_1 can be used as a follows. When the slow-exchange limit applies to both the T_1 and T_2 data, Equation 3 shows that s_1 and s_2 both equal k, and the ratio s_2/s_1 is one. When the fast-exchange limit applies to both relaxation times, one finds $s_2/s_1 = T_{2,p}^{-1}/T_{1,p}^{-1}$. Because in the present study $T_{2,p}^{-1}$ is at least 5–10 times larger than $T_{1,p}^{-1}$ (see below), the ratio of s_2 and s_1 is much larger than one in that case. It follows that when the value of s_2/s_1 is close to one, the slow-exchange limit applies to both T_1 and T_2 data and that, when this ratio becomes of the order of 5–10, the fast exchange limit pertains to the T_1 data and probably also to the T_2 data.

Different Protons—Protons located at different distances from the paramagnetic center will experience different magnetic interactions with the unpaired electron. As a result, their values of $T_{i,p}^{-1}$ will differ. In the fast-exchange limit, where s_i is proportional to $T_{i,p}^{-1}$, different protons will therefore exhibit different values of s_i. On the other hand, in the slow-exchange limit, where $s_i = k$, different protons will exhibit the same slope s_i. Consequently, when equal slopes s_i are observed for two protons, the slow-exchange regime will apply to both of them; when the slopes differ significantly, at least for the proton exhibiting the smaller slope, the slow-exchange limit cannot obtain.

DISCUSSION

For the His-35 and His-46 protons under investigation here, the values of s_1 and s_2 as well as their ratios measured under various conditions have been presented in Table I. On the basis of the criteria mentioned above, the relaxation regimes have been deduced as indicated in the last columns of Table I.

It now appears that under nearly all conditions the slow-exchange limit applies to the T_2 data of the His-46 proton. The short distance of this proton to the paramagnetic center apparently leads to a sufficiently large $T_{2,p}^{-1}$ to satisfy the conditions in Equation 1a. On the other hand, for the His-35 proton the fast-exchange limit is seen to prevail, in most cases. Clearly, compared with the His-46 proton, the larger proton-electron distance weakens the electron-proton interaction sufficiently so that now the condition in Equation 1b is fulfilled instead of that in Equation 1a. To confirm that different limits apply to the His-35 and His-46 protons, an additional experiment was performed in which the concentration of paramagnetic species was kept constant ([Az$_{ox}$] ≈ 40 μM), and the total azurin concentration was varied by dilution from 4.5 to 1 mM. The results are presented in Fig. 4, where $[Az_t](T_i^{-1} - T_{i,r}^{-1})/[Az_{ox}]$ is plotted as a function of [Az$_t$]. According to Equation 2, straight lines should be obtained with slopes equal to k (slow-exchange limit) or to zero (fast-exchange limit). The results of Fig. 4 nicely confirm that the slow-exchange limit applies to the T_2 data of the His-46 proton (slope of (6.0 ± 0.3) × 10^5 M^{-1} s^{-1}) and the fast-exchange limit to the T_1 and T_2 data of the His-35 proton (1 × 10^3 M^{-1} s^{-1}).

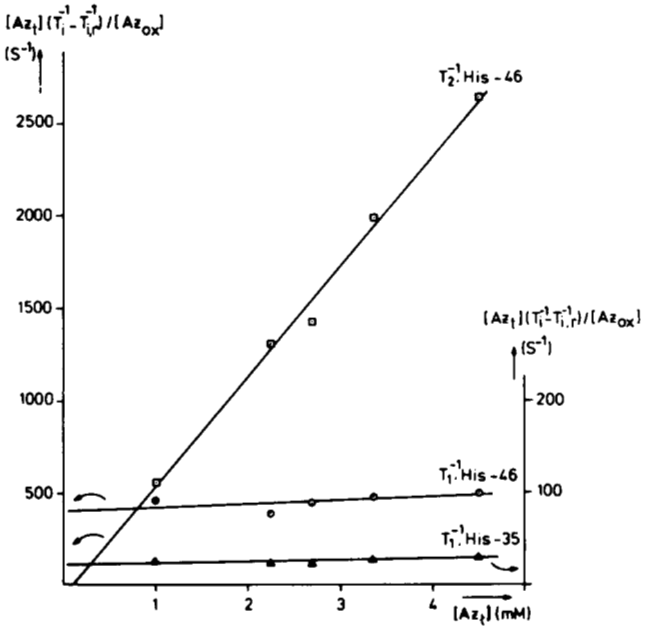

FIG. 4. **Plot of $[Az_t](T_i^{-1} - T_{i,r}^{-1})/[Az_{ox}]$ (s^{-1}) *versus* [Az$_t$] (mM) for His-35 (i = 1; △ and the His-46 proton (i = 1; ⊙ and i = 2; ⊡).** Experiments were performed at pH = 9.0 and 298 K. The oxidized azurin concentration was kept constant at approximately 40 μM, and the total azurin concentration was varied from 4.5 to 1 mM. *Right scale*, the T_1 data of the His-35 proton; *left scale*, the T_1 and T_2 data of the His-46 proton.

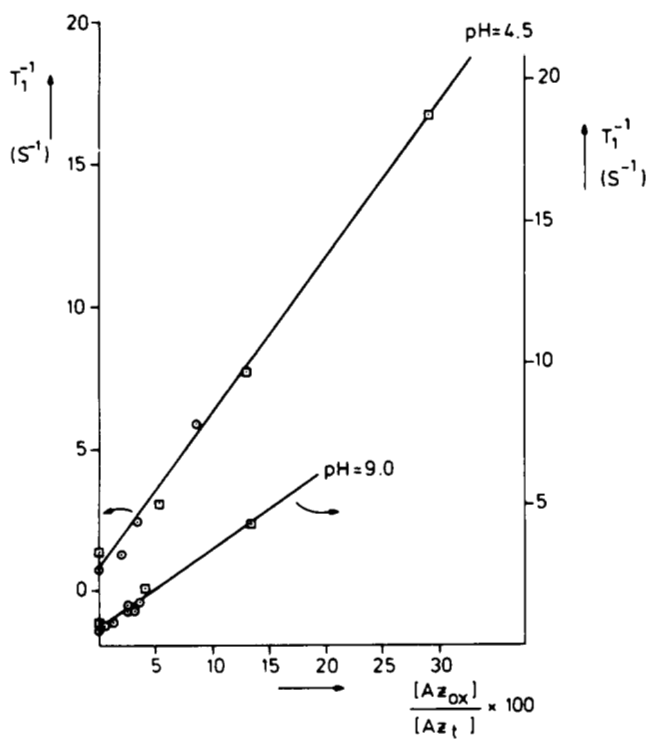

FIG. 5. **Plot of T_1^{-1} (s^{-1}) *versus* $[Az_{ox}]/[Az_t] \times 100$ for the His-35 proton.** Experiments were performed at pH 4.5 (*left scale*) and 9.0 (*right scale*), both at T = 298 K. Data at [Az$_t$] = 1 mM (⊙) were taken from the present study, and data at [Az$_t$] = 4.5 mM (⊡) were taken from the literature (Ugurbil and Mitra, 1985).

(In passing, it is pointed out that, qualitatively, the difference in relaxation behavior between these two protons is also immediately obvious from inspection of the experimental spectra (see Figs. 1 and 2)).

In the past, the T_1 data of this His-35 proton have been analyzed in the slow-exchange limit, leading to incorrect values of the self-exchange rate constant on the order of 10^4 M^{-1} s^{-1} (Ugurbil and Mitra, 1985). It appears that application of the correct limit to these data leads to results that are consistent with the present study. A convenient way to demonstrate this is to plot the T_1^{-1} values of the His-35 proton as a function of $[Az_{ox}]/[Az_t]$. According to Equation 2b, the points should fall on a straight line, with slope $T_{1,p}^{-1}$, when the fast-exchange limit applies. In Fig. 5, the results from the present study, obtained at $[Az_t] = 1$ mM, are shown together with the data reported by Ugurbil and Mitra (Ugurbil and Mitra, 1985) for $[Az_t] = 4.5$ mM. As is clearly seen from this figure, the results of the latter authors fit in nicely with the results of the present study, and the experimental points of both studies do indeed fall on a straight line.

The proper relaxation regime having been established, a numerical analysis of the data of Table I can now be performed. Values of the self-exchange rate constant can be extracted from the T_2 data of the His-46 proton, because here the slow-exchange limit applies and $k = s_2$. These values have been collected in Table II, together with literature values of k (Groeneveld and Canters, 1985a, 1985b; Groeneveld *et al.*, 1987). Table II shows that the values obtained in the present study exhibit good agreement with earlier reported values.

TABLE II

Electron self-exchange rate constants of azurin at different temperatures and pH values

T	pH	$k \times 10^{-6}$		
K		M^{-1} s^{-1}		
277	5.0			6.1 (2.6)[a]
	9.0			3.2 (0.7)[a]
298	4.5	9.6 (0.7)[b]	4.1 (0.7)[c]	
	9.0	5.8 (0.4)[b]	5.6 (0.8)[c]	
		6.0 (0.3)[b,d]		
320	4.5	30 (10)[b,e]	31 (10)[c]	
	9.0	10 (1)[b]	18 (3)[c]	

[a] Data from Groeneveld *et al.*, 1987.
[b] This study; values obtained from the slopes s_2 of the His-46 proton (Table I). The value at pH = 9.0 (298 K) is a weighted average of the 1 and 4.5 mM data.
[c] Data from Groeneveld and Canters, 1985a, 1985b.
[d] Calculated from the dilution experiment (see the Text).
[e] Estimated error.

When the fast-exchange limit applies, values of $T_{i,p}^{-1}$ can be obtained from the data of Table I by multiplying s_i with the total azurin concentration. Values of $T_{i,p}^{-1}$ obtained in this way have been collected in Table III. In addition, the slopes of the regression lines in Fig. 5 directly provide values of $T_{i,p}^{-1}$ (see Equation 2b); they are also presented in Table III.

The His-35 data in Table III are considered first. As a result of the relatively large distance between the copper and the His-35 proton, $T_{i,p}^{-1}$ is governed entirely by the electron-nuclear dipolar interaction (no Fermi-contact interaction). The appropriate versions of the Solomon-Bloembergen equations for the nuclear relaxation rates are given by (Solomon and Bloembergen, 1956; Dwek, 1973)

$$T_{1,d}^{-1} = \frac{3}{10} \frac{\gamma_I^2 \gamma_e^2 \hbar^2}{r^6} \frac{\tau_c}{1 + \omega_I^2 \tau_c^2} \tag{4a}$$

$$T_{2,d}^{-1} = \frac{1}{20} \frac{\gamma_I^2 \gamma_e^2 \hbar^2}{r^6} \left(4\tau_c + \frac{3\tau_c}{1 + \omega_I^2 \tau_c^2} \right) \tag{4b}$$

in which $T_{1,d}^{-1}$ denotes the contribution from the electron-nuclear dipolar interaction to the proton relaxation, τ_c denotes the corresponding correlation time, and r denotes the electron-nucleus distance. The other symbols have their usual meaning (Dwek, 1973). By equating $T_{i,p}^{-1}$ from Table III to $T_{i,d}^{-1}$, values of r and τ_c were calculated. The results are presented in the last columns of Table III. It is found that the correlation time τ_c varies from 1.0 to 2.4 ns, with an average of 1.6 ns. Although τ_c is a composite of the electron spin and rotational correlation times ($\tau_c^{-1} = \tau_e^{-1} + \tau_r^{-1}$), it is dominated by τ_e in the present case, τ_r being of the order of 5–10 ns (Canters *et al.*, 1984a).

The values found for r range from 0.76 to 0.90 nm and are larger than expected on the basis of crystallographic data (0.63 nm (Adman *et al.*, 1978; Adman and Jensen, 1981)). Interestingly, there is a pH effect on $T_{i,p}^{-1}$. This is clearly seen, for instance, as a difference in slope of the plots in Fig. 5. The most natural explanation is that the copper-proton distance, r, is affected by pH. An increase in r of about 11% (or 0.08 nm) upon an increase of pH from 4.5 to 9.0 would be sufficient to explain the experimental observations. This is a substantial change and confirms a previous deduction from NMR experiments that His-35 undergoes a significant change in position upon a change of pH (Adman *et al.*, 1982, 1983).

The data also clarify why the slow-exchange limit was mistakenly invoked previously (Ugurbil and Mitra, 1985) for the analysis of the T_1 data of the His-35 proton. To check the condition in Equation 1a, $T_{i,p}^{-1}$ was estimated by inserting the crystallographic value of 0.6 nm for r in Equation 4a. In the

TABLE III

Analysis of relaxation data obtained in the fast-exchange limit

	T	pH	$[Az_t]$	$T_{1,p}^{-1a}$	$T_{2,p}^{-1a}$	τ_c	r
	K		mM	s^{-1}		ns	nm
His-35	298	4.5	1	62 (6)	230 (24)	1.0 (0.1)	0.80 (0.02)
				55 (2)[b]			
		9.0	1	27 (3)	120 (40)	1.2 (0.3)	0.90 (0.03)
			4.5	25 (6)	270 (80)	2.0 (0.4)	0.85 (0.05)
				28 (1)[b]			
	320	4.5	1	60 (3)	480 (70)	1.7 (0.2)	0.76 (0.01)
		9.0	4.5	25 (4)	360 (230)	2.4 (0.9)	0.83 (0.06)
His-46	298	9.0	4.5	495 (45)			0.54 (0.01)[c]
	320	4.5	1	600 (250)			0.52 (0.04)[c]
		9.0	4.5	495 (45)	4500 (140)		

[a] Obtained from the slopes s_1 and s_2 in Table I multiplied by the total azurin concentration (see Equation 3b).
[b] Obtained from slopes of the plots in Fig. 5 (see Equation 2b and text).
[c] Calculated by using $\tau_c = 1.6$ ns.

ensuing calculation, the error in the distance was amplified, because of the 6th power appearance of r in Equation 4a, which led to an overestimate of $T_{i,p}^{-1}$ by an order of magnitude, eventually.

The His-46 T_2 data are of special interest because potentially they contain information on the magnitude of a Fermi-contact interaction. First, the T_1 data are considered. The contribution of the Fermi-contact interaction to $T_{i,p}^{-1}$ is negligible (Canters *et al.*, 1984a), and $T_{1,p}^{-1}$ can be equated to $T_{1,d}^{-1}$ for the His-46 proton. Inserting the average value of 1.6 ns for τ_c in Equation 4a, values of the electron-proton distance of 0.52 and 0.54 nm are found (see Table III). The His-46 signal has been assigned to the $C_{\delta 2}$-proton (Canters *et al.*, 1984b). In the crystal structure, the distance from this proton to the copper ion amounts to 0.54 nm, in nice agreement with the values of r found here.

One entry in Table III reports values for both $T_{1,p}^{-1}$ and $T_{2,p}^{-1}$ of the His-46 proton (320 K, pH 9.0, and $[Az_t] = 4.5$ mM). When inserting $\tau_c = 1.6$ ns and $r = 0.54$ nm into equation 4, a and b, one finds $T_{1,d}^{-1} = 475\ s^{-1}$ and $T_{2,d}^{-1} = 3420\ s^{-1}$. The calculated $T_{1,d}^{-1}$ value accounts approximately for the experimental value of $T_{1,p}^{-1}$ reported in Table III, but for $T_{2,p}^{-1}$ there is a residual contribution of $1080\ s^{-1}$. When assuming this is due to the Fermi-contact interaction, the magnitude of the latter can be calculated from the corresponding expression for the line width contribution $T_{2,Fc}^{-1} = \frac{A^2}{4}\tau_e$, in which A is related to the hyperfine splitting constant a, expressed in gauss, by $A = \gamma_e a$. When inserting $\tau_e = 1.6$ ns and $T_{2,Fc}^{-1} = 1080\ s^{-1}$, the calculated value of the hyperfine splitting constant a amounts to 85 mG. This is a perfectly acceptable value (Canters *et al.*, 1984a). Although the accuracy of the data is insufficient at present to establish the magnitude of the Fermi-contact interaction with certainty, it is unlikely that the hyperfine splitting constant appreciably exceeds a value of 100 mG.

CONCLUSION

The analysis of the paramagnetic effects in a ^1H NMR spectrum caused by an electron self-exchange reaction is straightforward and relatively simple in either the slow- or fast-exchange limit. However, a careful analysis of the effects of temperature and concentration on the paramagnetic broadening, preferably of more than one proton signal, is necessary to establish whether one of these limits applies.

The present study demonstrates that when values of the exchange rate have been determined in the slow-exchange limit, internal consistency of the analysis does not necessarily ensure its correctness (Ugurbil and Mitra, 1985). It is also clear that use of the Solomon-Bloembergen equations in combination with crystallographic data to check the conditions for slow or fast exchange may easily lead to erroneous results if no attention is paid to the reliability of the crystallographic data. Small errors are amplified because of the r^{-6} dependence in the line width expression (Ugurbil and Mitra, 1985).

The present study has unequivocally demonstrated that the electron self-exchange rate of *P. aeruginosa* azurin is surprisingly fast ($k \approx 10^6\ M^{-1}\ s^{-1}$ at room temperature) and that its rate is independent of pH ($5 < pH < 9$). This is all the more remarkable because conformational effects in the vicinity of His-35, brought about by variations in pH (Adman *et al.*, 1982, 1983; Canters *et al.*, 1984b), are found here to be on the order of about 1 Å. On the other hand, other groups have shown that the electron transfer reaction of azurin with various redox proteins definitively depends upon pH (Silvestrini *et al.*, 1981, 1986). A natural explanation for these observations is the presence of different electron transfer sites on the azurin surface (Farver and Pecht, 1981a; Farver *et al.*, 1982). The employment of a site close to His-35 (Farver *et al.*, 1982) in the reaction with the different partners would explain the observed pH dependence of the reaction rates. The location of the second site is discussed below.

For the structurally similar plastocyanins, it has been argued elsewhere that two patches on the surface may function as electron transfer sites, one close to Tyr-83 and residues 42–45, rather far away from the copper, and the second one located around ligand His-83 and known as the hydrophobic patch (Farver and Pecht, 1981b; Chapman *et al.*, 1983; Sykes, 1985). A similar hydrophobic patch can be recognized on the azurin surface around ligand His-117. On the basis of thermodynamic considerations and the observed independence of the self-exchange rate on ionic strength, it has been argued that the hydrophobic patch plays a crucial role in the azurin self-exchange reaction (Groeneveld and Canters, 1985a). When two azurin molecules "dock" along their hydrophobic patches, the copper-copper distance happens to attain its minimum possible value of about 14 Å. The question then is how electron transfer can be effected over such a large distance at the apparently high rate of $10^6\ M^{-1}\ s^{-1}$. When applying the equations corresponding with the case of nonadiabatic electron transfer to the analysis of the self-exchange rate data (Groeneveld and Canters, 1985a), it is found that a self-exchange rate of the order of $10^6\ M^{-1}\ s^{-1}$ is compatible only with an electron transfer distance of about 6–7 Å. In this respect, the packing of the azurin molecules in the crystal is suggestive (Adman *et al.*, 1978; Adman and Jensen, 1981; Norris *et al.*, 1983). One of the contact areas between two molecules happens to consist of the hydrophobic patches on the two protein surfaces. The His-117 ligands, which slightly protrude through this surface, appear to be oriented parallel to each other, with the edges of their imidazole rings about 7 Å apart. When a configuration like this would occur in solution, it would promote overlap of π-electron densities and optimize chances for electron exchange. The imidazole rings would act as bridges that would close, in part, the gap between the copper atoms, and the distance between their edges would be consistent with theoretical estimates of the electron transfer distance.

In summary, the following conclusions can therefore be stated: 1) A change in pH causes sizable conformational changes in the neighborhood of His-35. 2) The experimental data on the azurin self-exchange and the electron exchange of azurin with different redox proteins are compatible with the existence of two electron transfer sites on the protein surface. 3) The hydrophobic patch is probably involved in the electron self-exchange reaction. 4) The high self-exchange rate points to a bridging role of the His-117 ligands in the azurin electron transfer reaction.

Acknowledgments—We thank Dr. L. F. Oltmann for instructions concerning the microbiology and the growing of *P. aeruginosa* bacteria and Prof. Dr. J. Reedijk for the critical reading of the manuscript.

REFERENCES

Adman, E. T. & Jensen, L. H. (1981) *Isr. J. Chem.* **21,** 8–12
Adman, E. T., Stenkamp, R. E., Sieker, L. C. & Jensen, L. H. (1978) *J. Mol. Biol.* **123,** 35–47
Adman, E. T., Canters, G. W., Hill, H. A. O. & Kitchen, N. A. (1982) *FEBS Lett.* **143,** 287–292
Adman, E. T., Canters, G. W., Hill, H. A. O. & Kitchen, N. A. (1983) *Inorg. Chim. Acta* **79,** 127–128
Ambler, R. P. (1963) *Biochem. J.* **89,** 341–349
Beattie, J. K., Fensom, D. J., Freeman, H. C., Woodcock, E., Hill, H.

A. O. & Stokes, A. M. (1975) *Biochim. Biophys. Acta* **405,** 109–114
Canters, G. W. & Groeneveld, C. M. (1986) in *Frontiers in Bioinorganic Chemistry* (Xavier, A. V., ed) pp. 694–703, VCH Verlagsgesellschaft mbH, Weinheim, FRG
Canters, G. W., Hill, H. A. O., Kitchen, N. A. & Adman, E. T. (1984a) *J. Magn. Reson.* **57,** 1–23
Canters, G. W., Hill, H. A. O., Kitchen, N. A. & Adman, E. T. (1984b) *Eur. J. Biochem.* **138,** 141–152
Chapman, S. K., Watson, A. D. & Sykes, A. G. (1983) *J. Chem. Soc. Dalton Trans.* 2543–2548
Cho, K. C., Blair, D. F., Banerjee, U., Hopfield, J. J., Gray, H. B., Pecht, I. & Chan, S. I. (1984) *Biochemistry* **23,** 1858–1862
Concar, D. W., Hill, H. A. O., Moore, G. R., Whitford, D. & Williams, R. J. P. (1986) *FEBS Lett.* **206,** 15–19
Corin, A. F., Bersohn, R. & Cole, P. E. (1983) *Biochemistry* **22,** 2032–2038
Dahlin, S., Reinhammar, B. & Wilson, M. T. (1984) *Biochem. J.* **218,** 609–614
Dwek, R. A. (1973) *Nuclear Magnetic Resonance in Biochemistry: Applications to Enzyme Systems,* Oxford University Press, Oxford and New York
Farver, O. & Pecht, I. (1981a) *Isr. J. Chem.* **21,** 13–17
Farver, O. & Pecht, I. (1981b) *Proc. Natl. Acad. Sci. U. S. A.* **78,** 4190–4193
Farver, O. & Pecht, I. (1981c) in *Metal Ions in Biology: Copper Proteins* (Spiro, T. G., ed) pp. 151–192, John Wiley & Sons, New York
Farver, O., Blatt, Y. & Pecht, I. (1982) *Biochemistry* **21,** 3556–3561
Goldberg, M. & Pecht, I. (1976) *Biochemistry* **15,** 4197–4208
Groeneveld, C. M. & Canters, G. W. (1985a) *Eur. J. Biochem.* **153,** 559–564
Groeneveld, C. M. & Canters, G. W. (1985b) *Rev. Port. Quim.* **27,** 145
Groeneveld, C. M., Dahlin, S., Reinhammar, B. & Canters, G. W. (1987) *J. Am. Chem. Soc.* **109,** 3247–3250
Gupta, R. K., Koenig, S. H. & Redfield, A. G. (1972) *J. Magn. Reson.* **7,** 66–73
Keller, R. M. & Wüthrich, K. (1976) *FEBS Lett.* **70,** 180–184
McLaughlin, A. C. & Leigh, J. S., Jr. (1973) *J. Magn. Reson.* **9,** 296–304
Marcus, R. A. (1963) *J. Phys. Chem.* **67,** 853–857
Norris, G. E., Anderson, B. F. & Baker, E. N. (1983) *J. Mol. Biol.* **165,** 501–521
Parr, S. R., Barber, D., Greenwood, C., Phillips, B. W. & Melling, J. (1976) *Biochem. J.* **157,** 423–430
Silvestrini, M. C., Brunori, M., Wilson, T. & Darley-Usmar, V. (1981) *J. Inorg. Chem.* **14,** 327–338
Silvestrini, M. C., Brunori, M., Tegoni, M., Gervais, M. & Labeyrie, F. (1986) *Eur. J. Biochem.* **161,** 465–472
Solomon, I. & Bloembergen, N. (1956) *J. Chem. Phys.* **25,** 261–266
Sykes, A. G. (1985) *Chem. Soc. Rev.* **14,** 283–316
Ugurbil, K. & Mitra, S. (1985) *Proc. Natl. Acad. Sci. U. S. A.* **82,** 2039–2043